

Effect of Rare-earth Element Substitution in Superconducting $R_3Ni_2O_7$ Under Pressure

Zhiming Pan,^{1,2,*} Chen Lu,^{2,*} Fan Yang,^{3,†} and Congjun Wu^{2,1,4,5,‡}

¹*Institute for Theoretical Sciences, Westlake University, Hangzhou 310024, Zhejiang, China*

²*New Cornerstone Science Laboratory, Department of Physics,*

School of Science, Westlake University, Hangzhou 310024, Zhejiang, China

³*School of Physics, Beijing Institute of Technology, Beijing 100081, China*

⁴*Key Laboratory for Quantum Materials of Zhejiang Province,*

School of Science, Westlake University, Hangzhou 310024, Zhejiang, China

⁵*Institute of Natural Sciences, Westlake Institute for Advanced Study, Hangzhou 310024, Zhejiang, China*

Recently, high temperature ($T_c \approx 80K$) superconductivity (SC) has been discovered in $La_3Ni_2O_7$ (LNO) under pressure. Question arises whether the transition temperature T_c could be further enhanced under suitable conditions. A possible route for realizing higher T_c is element substitution. Similar SC could appear in rare-earth (RE) $R_3Ni_2O_7$ (RNO, R=RE element) material series under pressure. The electronic properties in the RNO materials are dominated by the Ni $3d$ orbitals in the bilayer NiO_2 plane. In the strong coupling limit, the SC could be fully characterized by a bilayer single $3d_{x^2-y^2}$ -orbital t - J_{\parallel} - J_{\perp} model. Under RE element substitution from La to RE element, the lattice constant decreases and the electronic hopping increases, leading to stronger superexchanges between the $3d_{x^2-y^2}$ orbitals. Based on the slave-boson mean-field theory, we explore the pairing nature and the evolution of T_c in RNO materials. Consequently, it is found that the element substitution does not alter the pairing nature, i.e. the inter-layer s -wave pairing is always favored in RNO. However, the T_c increases from La to Sm and a nearly doubled T_c is achieved for SmNO. This work provides evidence for possible higher T_c $R_3Ni_2O_7$ materials, which may be realized in further experiments.

Introduction The recent discovered high-temperature superconductivity in $La_3Ni_2O_7$ (LNO) [1] has attracted great interests both experimentally [2–6] and theoretically [7–33]. The signature of the superconducting transition temperature T_c is about 80K under pressures over 14GPa [1], which manifests as a newly platform of studying high- T_c superconductor other than cuprates [34, 35].

The basic ingredient for the electronic properties in LNO is the bilayer NiO_2 planes [1]. On average, each $Ni^{2.5+}$ is half-filled in its $3d_{z^2}$ orbital and quarter-filled in its $3d_{x^2-y^2}$ orbital. The spin alignment in the two E_g orbitals is further restricted from the Hund's rule. The $3d_{z^2}$ electrons could hop between the two NiO_2 layers through the intermediate $O2p_z$ orbitals, while the $3d_{x^2-y^2}$ electrons mostly hop within the layers. The physical filling of the two E_g orbitals could deviate due to the self-doped effect from hybridization between them [25, 27] or doping of holes on the $O2p$ orbitals[16].

Taken into account the Hund's rule, we have suggested an effective bilayer single- $3d_{x^2-y^2}$ orbital t - J_{\parallel} - J_{\perp} model as the minimal model for the high- T_c superconductivity in the strong coupling limit [20]. Each NiO_2 layer is composed by a conventional t - J_{\parallel} model with nearest-neighbor intra-layer antiferromagnetic (AFM) spin exchange J_{\parallel} . The two NiO_2 layers couple through an effective inter-layer AFM spin exchange J_{\perp} between $3d_{z^2}$

electrons lying on the two layers, which is generated from integrating out the $3d_{z^2}$ orbital degrees of freedom under the strong Hund's coupling. The superconducting transition temperature could be dramatically enhanced when the inter-layer coupling J_{\perp} is larger than the intra-layer one[20]. This kind of bilayer t - J model has already been explored in multilayer cuprates [36–40] and may be realized recently in ultracold atoms [41–43]. Most of these works focus on the theoretical side with different physical parameter regime [36–47]. The strong interlayer coupling J_{\perp} in LNO plays important role for high T_c [20], which is hard to be realized in multilayer cuprates.

Effect of element substitution is an important chemical approach to increase the superconducting transition temperature. Replacing the La element by other rare-earth (RE) elements could influence the crystal and electronic structure of the materials. Elements substitution alters the lattice constant, modifying the hopping strength of electrons. Under suitable pressure, $R_3Ni_2O_7$ (RNO, R=RE elements) material series undergo similar structure transition to the Fmmm phase as LNO [27], opening up the possibility of realizing high T_c in these materials.

Previous first principle density functional theory (DFT) for $R_3Ni_2O_7$ reveals the RE elements dependence of the physical parameters[27]. The hopping strength could be enhanced through element substitution. However, the weak coupling analysis based on random phase approximation (RPA) predicts that the pairing strength is reduced from La to Sm, and the superconducting transition temperature T_c decreases simultaneously [27]. Such calculation might suggest that LNO already has the

* These two authors contributed equally to this work.

† yangfan_blg@bit.edu.cn

‡ wucongjun@westlake.edu.cn

largest T_c in the RNO material series.

The situation could be reversed in the strong coupling picture, where T_c is related to the superexchange strength J_\perp [20]. Based on the hopping strength from the DFT calculations [27], the effective AFM couplings J_\perp and J_\parallel increase simultaneously from La to Sm. Previous calculation has already seen that strong super-exchange J_\perp could enhance the T_c , leading to the high- T_c observed in the LNO experiment [20]. All the relevant energy scales grow up under the element substitution. These observations provide potential increased T_c under elements substitution.

In this work, we study the effect of RE element substitution in RNO materials based on the effective bilayer single $3d_{x^2-y^2}$ -orbital t - J_\parallel - J_\perp model[20]. We first obtain the effective AFM spin exchange J_\perp and J_\parallel for different RE elements from the DFT calculation[27]. Then, we apply the slave-boson mean field analysis [48, 49] for the bilayer t - J model within these physical parameters. The superconducting pairing gaps and transition temperatures T_c are numerical calculated. Our results suggest that the element substitution does not change the pairing nature, i.e. the inter-layer s-wave pairing. However, the T_c could be strongly enhanced through element substitution in this strong coupling scenario, and especially from La to Sm, T_c nearly doubles. This work provides possible route for enhancing T_c and appeals for experimental verification.

Effective bilayer model In the double-layered Ruddlesden-Popper $R_3\text{Ni}_2\text{O}_7$ material, electronic properties are decoded in the bilayer NiO_2 planes. DFT calculation [1, 27, 50] indicates that the relevant physical degrees of freedom come from the two E_g orbital in $\text{Ni}^{2.5+}$, where $3d_{z^2}$ orbital is half-filled and $3d_{x^2-y^2}$ orbital is quarter-filled. The inter-layer hopping t_{zz}^\perp between the $3d_{z^2}$ orbitals and the intra-layer hopping t_{xx}^\parallel between the $3d_{x^2-y^2}$ orbitals dominate the mobile electron process. In the strong coupling limit with large Hubbard- U ($U \simeq 4\text{eV}$), an effective inter-layer spin superexchange for $3d_{z^2}$ orbitals and intra-layer one for $3d_{x^2-y^2}$ orbitals are generated,

$$J_\perp = \frac{4t_{zz}^{\perp 2}}{U}, \quad J_\parallel = \frac{4t_{xx}^{\parallel 2}}{U}. \quad (1)$$

Moreover, J_\perp is larger than J_\parallel due to the larger inter-layer hopping of $3d_{z^2}$ orbitals.

The relevant physics in RNO is described by a bilayer two-orbital t - J - J_H model,

$$\begin{aligned} H = & -t_{xx}^\parallel \sum_{\langle i,j \rangle \alpha \sigma} (d_{x^2 i \alpha \sigma}^\dagger d_{x^2 j \alpha \sigma} + \text{h.c.}) \\ & + J_\parallel \sum_{\langle i,j \rangle \alpha} \mathbf{S}_{x^2 i \alpha} \cdot \mathbf{S}_{x^2 j \alpha} \\ & + J_\perp \sum_i \mathbf{S}_{z^2 i 1} \cdot \mathbf{S}_{z^2 i 2} - J_H \sum_{i \alpha} \mathbf{S}_{x^2 i \alpha} \cdot \mathbf{S}_{z^2 i \alpha}, \quad (2) \end{aligned}$$

where $d_{x^2 i \alpha \sigma}^\dagger$ is electron creation operator for $3d_{x^2-y^2}$ orbital at the lattice site i , $\alpha = 1, 2$ is the layer index

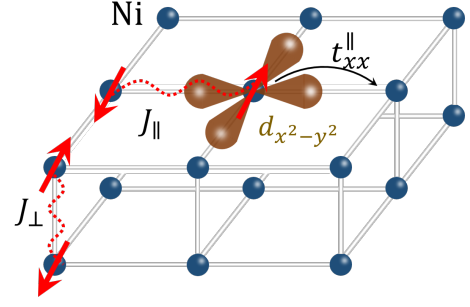


FIG. 1. Schematic diagram for the effective single $3d_{x^2-y^2}$ orbital bilayer t - J_\parallel - J_\perp model. Each layer is comprised by a conventional intra-layer t - J_\parallel model, while the two layers interact through an inter-layer spin exchange J_\perp .

for the two NiO plane and $\sigma = \uparrow, \downarrow$ is the spin index. $\mathbf{S}_{x^2 i \alpha} = \frac{1}{2} d_{x^2 i \alpha}^\dagger [\boldsymbol{\sigma}] d_{x^2 i \alpha}$ is the spin operator for $3d_{x^2-y^2}$ electron, with Pauli matrix $\boldsymbol{\sigma} = (\sigma_x, \sigma_y, \sigma_z)$. The summation $\sum_{\langle i,j \rangle}$ takes over all the nearest neighbor sites i, j within the plane. $\mathbf{S}_{z^2 i \alpha}$ is the spin operator for the localized $3d_{z^2}$ orbital. The two orbitals interact through the strong on-site Hund's coupling J_H .

The effective minimal model under strong Hund's coupling is a bilayer t - J_\parallel - J_\perp model for the single $3d_{x^2-y^2}$ orbital[20]. The strong Hund's coupling binds the spins of $3d_{x^2-y^2}$ and $3d_{z^2}$ orbitals into a spin-triplet state. The inter-layer $3d_{z^2}$ spin exchange J_\perp will be transmitted to $3d_{x^2-y^2}$ spins, generating an effective inter-layer spin exchange J_\perp between $3d_{x^2-y^2}$ spins. Integrating out the $3d_{z^2}$ degrees of freedom under strong Hund's coupling ($J_H \gg J_\perp$), the two-orbital system Eq. (2) reduces to the bilayer single $3d_{x^2-y^2}$ -orbital model,

$$\begin{aligned} H = & -t_{xx}^\parallel \sum_{\langle i,j \rangle \alpha \sigma} (d_{x^2 i \alpha \sigma}^\dagger d_{x^2 j \alpha \sigma} + \text{h.c.}) \\ & - t_{xx}^\perp \sum_{i \sigma} (d_{x^2 i 1 \sigma}^\dagger d_{x^2 i 2 \sigma} + \text{h.c.}) \\ & + J_\parallel \sum_{\langle i,j \rangle \alpha} \mathbf{S}_{x^2 i \alpha} \cdot \mathbf{S}_{x^2 j \alpha} + J_\perp \sum_i \mathbf{S}_{x^2 i 1} \cdot \mathbf{S}_{x^2 i 2}, \quad (3) \end{aligned}$$

with intra-layer nearest-neighbor AFM spin exchanges J_\parallel and inter-layer one J_\perp , as depicted in Fig. (1). A small inter-layer hopping t_{xx}^\perp is added, which could fix the relative phases between the pairings of the two layers. In the reduced model, $3d_{z^2}$ orbital plays as an intermediate hidden bridge for the inter-layer coupling J_\perp between $3d_{x^2-y^2}$ orbitals. It also accounts for the self-doping effect in the $3d_{x^2-y^2}$ orbital [25, 27].

The filling level x (or doping level $\delta = 1 - 2x$) of $3d_{x^2-y^2}$ orbital deviates from quarter filling due to the hybridization between the two E_g orbitals. C_4 rotation symmetry around the z -axis forbids the on-site hybridization between $3d_{z^2}$ and $3d_{x^2-y^2}$ orbital. However, symmetry arguments still persist a finite hybridization between neighbor sites. In the DFT calculation[7, 27], such nearest-

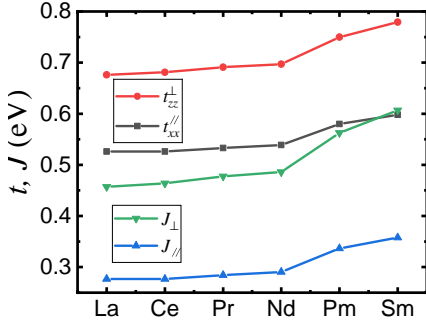


FIG. 2. Relevant hopping strength and effective spin exchange for different RE elements from La to Sm. From La to Sm, the inter-layer $3d_{z^2}$ hopping t_{zz}^\perp and intra-layer $3d_{x^2-y^2}$ hopping t_{xx}^\parallel both gradually increase [27]. The effective inter-layer $3d_{z^2}$ spin exchange J_\perp and intra-layer $3d_{x^2-y^2}$ spin exchange J_\parallel follow the similar tendency.

neighbor hybridization between $3d_{z^2}$ and $3d_{x^2-y^2}$ orbital has been shown to be comparable to the nearest-neighbor hopping in the RNO materials. The two orbitals mix together, leading to bonding or anti-bonding state. Moreover, an effective intra-layer hopping process could be generated for $3d_{z^2}$ orbital. The averaged densities of the $3d_{z^2}$ and $3d_{x^2-y^2}$ orbitals deviate from half filling and quarter filling owing to the density fluctuations. For the RE elements from La to Sm, $3d_{x^2-y^2}$ orbital nearly keeps the same physical filling $x \approx 0.3$ from the DFT calculation [27].

Slave boson mean field theory In the slave boson mean field theory [48, 49], the electron operator is represented as $d_{x^2i\alpha\sigma}^\dagger = f_{i\alpha\sigma}^\dagger b_{i\alpha}$, where $f_{i\alpha\sigma}^\dagger$ is the spinon creation operator and $b_{i\alpha}$ is the holon annihilation operator. The super exchange term can be decoupled in the hopping and pairing channel, i.e., for the inter-layer one,

$$\begin{aligned} & J_\perp \mathbf{S}_{x^2i1} \cdot \mathbf{S}_{x^2i2} \\ &= - \left[\chi_{i\perp} (f_{i1\uparrow}^\dagger f_{i2\uparrow} + f_{i1\downarrow}^\dagger f_{i2\downarrow}) + \text{h.c.} - \frac{8}{3J_\perp} |\chi_{i\perp}|^2 \right] \\ & \quad - \left[\Delta_{i\perp} (f_{i1\uparrow}^\dagger f_{i2\downarrow}^\dagger - f_{i1\downarrow}^\dagger f_{i2\uparrow}^\dagger) + \text{h.c.} - \frac{8}{3J_\perp} |\Delta_{i\perp}|^2 \right], \end{aligned} \quad (4)$$

and similar decomposition for the intra-layer super exchange. In the mean-field ansatz, the hopping and pairing order parameters are represented by their mean-field values [20],

$$\begin{aligned} \chi_{ij}^{(\alpha)} &= \frac{3}{8} J_\parallel \langle f_{j\alpha\uparrow}^\dagger f_{i\alpha\uparrow} + f_{j\alpha\downarrow}^\dagger f_{i\alpha\downarrow} \rangle \equiv \chi_{j-i}^{(\alpha)}, \\ \Delta_{ij}^{(\alpha)} &= \frac{3}{8} J_\parallel \langle f_{j\alpha\downarrow}^\dagger f_{i\alpha\uparrow} - f_{j\alpha\uparrow}^\dagger f_{i\alpha\downarrow} \rangle \equiv \Delta_{j-i}^{(\alpha)}, \\ \chi_{i\perp} &= \frac{3}{8} J_\perp \langle f_{i2\uparrow}^\dagger f_{i1\uparrow} + f_{i2\downarrow}^\dagger f_{i1\downarrow} \rangle \equiv \chi_{\perp}, \\ \Delta_{i\perp} &= \frac{3}{8} J_\perp \langle f_{i2\downarrow}^\dagger f_{i1\uparrow} - f_{i2\uparrow}^\dagger f_{i1\downarrow} \rangle \equiv \Delta_{\perp}. \end{aligned} \quad (5)$$

The holon will condense at low temperature and holon

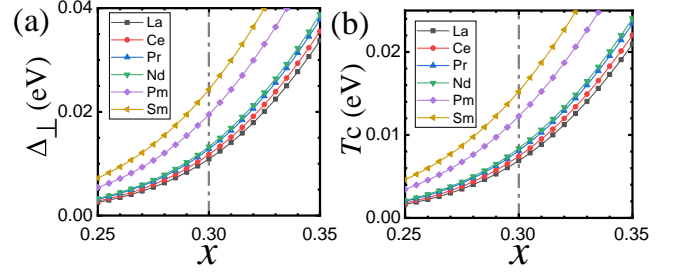


FIG. 3. (a). Inter-layer pairing gap Δ_\perp versus filling level x under element substitution for $R_3\text{Ni}_2\text{O}_7$ (R =rare-earth element from La to Sm). The place of physical filling $x \approx 0.3$ is shown in a dashed-dotted line. The superconducting gap increases as the filling level grows. (b). Superconducting transition temperature T_c versus filling level x under element substitution for $R_3\text{Ni}_2\text{O}_7$ (R =rare-earth element). From La to Sm element substitution, the pairing strength Δ_\perp and the superconducting T_c in RNO series increase simultaneously.

operators can be replaced by the condensation density, $b_{i\alpha} \sim b_{i\alpha}^\dagger \sim \sqrt{\delta} = \sqrt{1-2x}$.

The superconducting state is achieved when the spinon is paired and the holon is condensed[48]. There exist two typical temperature scales, T_{BEC} for the holon condensation, and T_{BCS} for the spinon pairing. The doping dependence of them differs from each other. T_{BEC} increases almost linearly as the doping level δ increase, which is typical very large near quarter filling. The spinon pairing temperature sets up as the superconducting temperature, $T_c = T_{\text{BCS}}$. While there exist pseudogap phase in high- T_c cuprates [35, 48], such phase is absent in the RNO materials since $T_{\text{BCS}} < T_{\text{BEC}}$.

RE element substitution Under the RE element substitution from La to Sm, the lattice constants decrease and the overlaps of neighbor electronic orbitals increase. Both the intra-layer $3d_{x^2-y^2}$ orbital hopping and inter-layer $3d_{z^2}$ one will gradually increase. On the contrary, the on-site Hubbard U interaction does not changes much. We adopt the hopping strength and Hubbard $U \simeq 4\text{eV}$ from the DFT calculations in the Ref. [27] for different RE elements. The effective inter-layer and intra-layer AFM spin super exchange are obtained from Eq. (1), as depicted in Fig. (2). J_\perp and J_\parallel increase from La to Sm, while their ratio nearly unchanged, $J_\perp/J_\parallel \approx 1.65 - 1.70$. Especially, for element substitution of Pm or Sm, the hopping strength and spin exchange get stronger much. Upon the RE element substitution, all the relevant energy scales become enhanced simultaneously, raising up the possibility of increased T_c .

In the relevant parameter regime, an inter-layer s -wave pairing with high T_c is deduced for RNO materials, similar as in LNO [20]. The superconducting state is dominated by the inter-layer $3d_{x^2-y^2}$ orbital s -wave pairing Δ_\perp , where the intra-layer one $\Delta_\mu^{(\alpha)}$ ($\mu = x, y$ and $\alpha = 1, 2$) nearly vanishes. Such a strong inter-layer pairing is a direct consequence of the large inter-layer

superexchange J_{\perp} compared to intra-layer one J_{\parallel} . The inter-layer pairings Δ_{\perp} from La to Sm elements grow up as the filling level increases, as depicted in Fig 3(a). The increased inter-layer pairing indicates possible higher BCS pairing temperature from element substitution.

The strong inter-layer superexchange J_{\perp} enhances the transition temperature dramatically, leading to the possible high T_c superconductivity in the RNO materials. The superconducting T_c for RNO is numerically estimated as a function of the filling level x , as depicted in Fig. 3(b). As x increases from quarter filling ($x = 0.25$), the transition temperature tends to increase monotonically. At the same time, from La to Sm element substitution, the transition temperature is enhanced for the same filling level and get a significant jump from element substitution of La to Pm or Sm. Such a strong enhancement in the temperature T_c results from the enhancement of the energy scales for Pm and Sm element, as already been seen clearly in Fig. (2). Moreover, the ratio between the pairing gap Δ_{\perp} and superconducting T_c is approximately $\Delta_{\perp}/T_c \approx 0.4/0.25 = 1.6$, which is quantitatively consistent with the prediction of BCS-type theory.

At the physical filling $x \approx 0.3$, the superconducting T_c nearly doubles from La to Sm element. It is expected that $\text{Sm}_3\text{Ni}_2\text{O}_7$ is the optimal material with the largest T_c in the RNO material series.

Discussion The superconducting pairing and T_c in the RNO materials are explored based on the bilayer single $3d_{x^2-y^2}$ orbital t - J_{\parallel} - J_{\perp} model. The numerical simulation shows that $\text{Sm}_3\text{Ni}_2\text{O}_7$ could exhibit the largest superconducting T_c . The scenario proposed here differs from previous weak coupling analysis based on RPA[27]. There, the pairing strength as well as superconducting temperature decrease from La to Sm element substitution, and LNO is already the optimal high- T_c material in the RNO series. In our strong coupling picture, the superconducting pairing is mainly generated from the effective inter-layer spin superexchange J_{\perp} . J_{\perp} naturally increases as the inter-layer hopping strength increases under RE element substitution, and the superconductivity would be enhanced.

As we emphasized in the previous work[20] and further confirmed in this work, the high- T_c superconductivity is driven by the strong interlayer spin exchange J_{\perp} for the $3d_{x^2-y^2}$ orbitals in the RNO candidates. The inter-layer s -wave superconducting pairing in the $3d_{x^2-y^2}$ orbital is favored in the relevant parameter regime, and the intra-layer hopping severs as the mobile engine. Such a situation is distinct from the d -wave pairing in the single-layer cuprate [48] and multilayer cuprates where the inter-layer exchange J_{\perp} is naturally smaller than J_{\parallel} [36–40]. The wavefunctions of $3d_{x^2-y^2}$ orbital nearly lie within the plane and the interlayer overlap between $3d_{x^2-y^2}$ orbitals is small. The strong $J_{\perp} > J_{\parallel}$ is hard to be directly

generated from the much smaller inter-layer hopping of single $3d_{x^2-y^2}$ orbitals compared to the intra-layer one. In the RNO materials, inter-layer overlap of $3d_{z^2}$ orbital wavefunctions persists strong inter-layer hopping. Strong J_{\perp} could be realized for $3d_{z^2}$ orbitals and is further transmitted to $3d_{x^2-y^2}$ orbitals under strong Hund's coupling.

Although we focus on the reduced single $3d_{x^2-y^2}$ orbital model, the effect of hidden $3d_{z^2}$ degrees of freedom plays an important role. $3d_{z^2}$ electrons are nearly localized within the plane and has strong inter-layer hopping, inducing the strong inter-layer super-exchange J_{\perp} . There also exist inter-layer pairings for the almost half-filled $3d_{z^2}$ orbitals. However, the inter-layer $3d_{z^2}$ pairings are also nearly localized. Even worse, $3d_{z^2}$ orbitals are nearly half-filled and holon condensation temperature is quite low due to its low density. $3d_{z^2}$ orbitals do not contribute to the superconducting transport behavior directly. On the contrary, the Hund's rule combines the two E_g orbitals into the spin-triplet states, and induces effective strong inter-layer couplings J_{\perp} between $3d_{x^2-y^2}$ orbitals.

While the simple single orbital model characterizes the most relevant physics of the superconducting LNO material [20], further theoretical work and experimental verification are necessary to understand the interplay between $3d_{x^2-y^2}$ and $3d_{z^2}$ orbitals. Moreover, the nature of the superconducting in $3d_{x^2-y^2}$ and $3d_{z^2}$ orbitals is different from each other. A comprehensive analysis takes into account both degrees of freedom will be helpful. Possible chemical doping approach may alter the superconducting behavior and further increase the T_c . We will leave these problems in the further works.

Conclusion In this work, we focus on the effect of RE element substitution to the high T_c superconductivity in the RNO materials under pressure based on the strong coupling bilayer single $3d_{x^2-y^2}$ orbital t - J_{\parallel} - J_{\perp} model. For the RE element from La to Sm, the effective inter-layer and intra-layer spin superexchange increase as the relevant hopping parameters grow up. In the relevant filling level, the superconducting T_c obtained is enhanced under the element substitution. Strikingly, T_c nearly doubles from substitution of La to Sm element, which might be experimental realized in the future. This works suggest that RE element substitution in RNO materials serves as an important approach to enhance the superconducting T_c , appealing for further experimental verification.

Acknowledgments F.Y. is supported by the National Natural Science Foundation of China under the Grants No. 12074031, No. 12234016, and No. 11674025. C.W. is supported by the National Natural Science Foundation of China under the Grants No. 12234016 and No. 12174317. This work has been supported by the New Cornerstone Science Foundation.

[1] H. Sun, M. Huo, X. Hu, J. Li, Z. Liu, Y. Han, L. Tang, Z. Mao, P. Yang, B. Wang, J. Cheng, D.-X. Yao, G.-

M. Zhang, and M. Wang, Signatures of superconductiv-

- ity near 80k in a nickelate under high pressure, *Nature* 10.1038/s41586-023-06408-7 (2023).
- [2] Z. Liu, M. Huo, J. Li, Q. Li, Y. Liu, Y. Dai, X. Zhou, J. Hao, Y. Lu, M. Wang, and H.-H. Wen, Electronic correlations and energy gap in the bilayer nickelate $\text{La}_3\text{Ni}_2\text{O}_7$, arXiv preprint arXiv:2307.02950 (2023).
- [3] J. Hou, P. T. Yang, Z. Y. Liu, J. Y. Li, P. F. Shan, L. Ma, G. Wang, N. N. Wang, H. Z. Guo, J. P. Sun, Y. Uwamoto, M. Wang, G. M. Zhang, B. S. Wang, and J. G. Cheng, Emergence of high-temperature superconducting phase in the pressurized $\text{La}_3\text{Ni}_2\text{O}_7$ crystals, arXiv preprint arXiv:2307.09865 (2023).
- [4] Y. Zhang, D. Su, Y. Huang, H. Sun, M. Huo, Z. Shan, K. Ye, Z. Yang, R. Li, M. Smidman, M. Wang, L. Jiao, and H. Yuan, High-temperature superconductivity with zero-resistance and strange metal behavior in $\text{La}_3\text{Ni}_2\text{O}_7$, arXiv preprint arXiv:2307.14819 (2023).
- [5] J. Yang, H. Sun, X. Hu, Y. Xie, T. Miao, H. Luo, H. Chen, B. Liang, W. Zhu, G. Qu, C.-Q. Chen, M. Huo, Y. Huang, S. Zhang, F. Zhang, F. Yang, Z. Wang, Q. Peng, H. Mao, G. Liu, Z. Xu, T. Qian, D.-X. Yao, M. Wang, L. Zhao, and X. J. Zhou, Orbital-dependent electron correlation in double-layer nickelate $\text{La}_3\text{Ni}_2\text{O}_7$, arXiv preprint arXiv:2309.01148 (2023).
- [6] M. Zhang, C. Pei, Q. Wang, Y. Zhao, C. Li, W. Cao, S. Zhu, J. Wu, and Y. Qi, Effects of pressure and doping on ruddlesden-popper phases, arXiv preprint arXiv:2309.01651 (2023).
- [7] Z. Luo, X. Hu, M. Wang, W. Wu, and D.-X. Yao, Bilayer two-orbital model of $\text{La}_3\text{Ni}_2\text{O}_7$ under pressure, arXiv preprint arXiv:2305.15564 (2023).
- [8] Y. Zhang, L.-F. Lin, A. Moreo, and E. Dagotto, Electronic structure, orbital-selective behavior, and magnetic tendencies in the bilayer nickelate superconductor $\text{La}_3\text{Ni}_2\text{O}_7$ under pressure, arXiv preprint arXiv:2306.03231 (2023).
- [9] Q.-G. Yang, D. Wang, and Q.-H. Wang, Possible s_{\pm} -wave superconductivity in $\text{La}_3\text{Ni}_2\text{O}_7$, arXiv preprint arXiv:2306.03706 (2023).
- [10] F. Lechermann, J. Gondolf, S. Bötzel, and I. M. Eremin, Electronic correlations and superconducting instability in $\text{La}_3\text{Ni}_2\text{O}_7$ under high pressure, arXiv preprint arXiv:2306.05121 (2023).
- [11] H. Sakakibara, N. Kitamine, M. Ochi, and K. Kuroki, Possible high T_c superconductivity in $\text{La}_3\text{Ni}_2\text{O}_7$ under high pressure through manifestation of a nearly-half-filled bilayer hubbard model, arXiv preprint arXiv:2306.06039 (2023).
- [12] Y. Gu, C. Le, Z. Yang, X. Wu, and J. Hu, Effective model and pairing tendency in bilayer ni-based superconductor $\text{La}_3\text{Ni}_2\text{O}_7$, arXiv preprint arXiv:2306.07275 (2023).
- [13] Y. Shen, M. Qin, and G.-M. Zhang, Effective bilayer model hamiltonian and density-matrix renormalization group study for the high- T_c superconductivity in $\text{La}_3\text{Ni}_2\text{O}_7$ under high pressure, arXiv preprint arXiv:2306.07837 (2023).
- [14] V. Christiansson, F. Petocchi, and P. Werner, Correlated electronic structure of $\text{La}_3\text{Ni}_2\text{O}_7$ under pressure, arXiv preprint arXiv:2306.07931 (2023).
- [15] D. Shilenko and I. Leonov, Correlated electronic structure, orbital-selective behavior, and magnetic correlations in double-layer $\text{La}_3\text{Ni}_2\text{O}_7$ under pressure, arXiv preprint arXiv:2306.14841 (2023).
- [16] W. Wú, Z. Luo, D.-X. Yao, and M. Wang, Charge transfer and zhang-rice singlet bands in the nickelate superconductor $\text{La}_3\text{Ni}_2\text{O}_7$ under pressure, arXiv preprint arXiv:2307.05662 (2023).
- [17] Y. Cao and Y.-F. Yang, Flat bands promoted by hund's rule coupling in the candidate double-layer high-temperature superconductor $\text{La}_3\text{Ni}_2\text{O}_7$, arXiv preprint arXiv:2307.06806 (2023).
- [18] X. Chen, P. Jiang, J. Li, Z. Zhong, and Y. Lu, Critical charge and spin instabilities in superconducting $\text{La}_3\text{Ni}_2\text{O}_7$, arXiv preprint arXiv:2307.07154 (2023).
- [19] Y.-B. Liu, J.-W. Mei, F. Ye, W.-Q. Chen, and F. Yang, The s_{\pm} -wave pairing and the destructive role of apical-oxygen deficiencies in $\text{La}_3\text{Ni}_2\text{O}_7$ under pressure, arXiv preprint arXiv:2307.10144 (2023).
- [20] C. Lu, Z. Pan, F. Yang, and C. Wu, Interlayer coupling driven high-temperature superconductivity in $\text{La}_3\text{Ni}_2\text{O}_7$ under pressure, arXiv preprint arXiv:2307.14965 (2023).
- [21] H. Oh and Y.-H. Zhang, Type II t - J model and shared antiferromagnetic spin coupling from hund's rule in superconducting $\text{La}_3\text{Ni}_2\text{O}_7$, arXiv preprint arXiv:2307.15706 (2023).
- [22] Y. Zhang, L.-F. Lin, A. Moreo, T. A. Maier, and E. Dagotto, Structural phase transition, s_{\pm} -wave pairing and magnetic stripe order in the bilayered nickelate superconductor $\text{La}_3\text{Ni}_2\text{O}_7$ under pressure, arXiv preprint arXiv:2307.15276 (2023).
- [23] Z. Liao, L. Chen, G. Duan, Y. Wang, C. Liu, R. Yu, and Q. Si, Electron correlations and superconductivity in $\text{La}_3\text{Ni}_2\text{O}_7$ under pressure tuning, arXiv preprint arXiv:2307.16697 (2023).
- [24] X.-Z. Qu, D.-W. Qu, J. Chen, C. Wu, F. Yang, W. Li, and G. Su, Bilayer t - J - J_{\perp} model and magnetically mediated pairing in the pressurized nickelate $\text{La}_3\text{Ni}_2\text{O}_7$, arXiv preprint arXiv:2307.16873 (2023).
- [25] Y.-F. Yang, G.-M. Zhang, and F.-C. Zhang, Minimal effective model and possible high- T_c mechanism for superconductivity of $\text{La}_3\text{Ni}_2\text{O}_7$ under high pressure, arXiv preprint arXiv:2308.01176 (2023).
- [26] K. Jiang, Z. Wang, and F.-C. Zhang, High temperature superconductivity in $\text{La}_3\text{Ni}_2\text{O}_7$, arXiv preprint arXiv:2308.06771 (2023).
- [27] Y. Zhang, L.-F. Lin, A. Moreo, T. A. Maier, and E. Dagotto, Trends of electronic structures and s_{\pm} -wave pairing for the rare-earth series in bilayer nickelate superconductor $R_3\text{Ni}_2\text{O}_7$, arXiv preprint arXiv:2308.07386 (2023).
- [28] J. Huang, Z. Wang, and T. Zhou, Impurity and vortex states in the bilayer high-temperature superconductor $\text{La}_3\text{Ni}_2\text{O}_7$, arXiv preprint arXiv:2308.07651 (2023).
- [29] Q. Qin and Y.-F. Yang, High- T_c superconductivity by mobilizing local spin singlets and possible route to higher T_c in pressurized $\text{La}_3\text{Ni}_2\text{O}_7$, arXiv preprint arXiv:2308.09044 (2023).
- [30] Y.-H. Tian, Y. Chen, J.-M. Wang, R.-Q. He, and Z.-Y. Lu, Correlation effects and concomitant two-orbital s_{\pm} -wave superconductivity in $\text{La}_3\text{Ni}_2\text{O}_7$ under high pressure, arXiv preprint arXiv:2308.09698 (2023).
- [31] R. Jiang, J. Hou, Z. Fan, Z.-J. Lang, and W. Ku, Pressure driven screening of Ni spin results in cuprate-like high- T_c superconductivity in $\text{La}_3\text{Ni}_2\text{O}_7$, arXiv preprint arXiv:2308.11614 (2023).
- [32] D.-C. Lu, M. Li, Z.-Y. Zeng, W. Hou, J. Wang, F. Yang, and Y.-Z. You, Superconductivity from doping symmetric mass generation insulators: Application to $\text{La}_3\text{Ni}_2\text{O}_7$

- under pressure, arXiv preprint arXiv:2308.11195 (2023).
- [33] Z. Luo, B. Lv, M. Wang, W. Wu, and D.-X. Yao, High- T_c superconductivity in $\text{La}_3\text{Ni}_2\text{O}_7$ based on the bilayer two-orbital tJ model, arXiv preprint arXiv:2308.16564 (2023).
- [34] J. G. Bednorz and K. A. Müller, Possible high T_c superconductivity in the ba- la- cu- o system, *Zeitschrift für Physik B Condensed Matter* **64**, 189 (1986).
- [35] C. Proust and L. Taillefer, The remarkable underlying ground states of cuprate superconductors, *Annual Review of Condensed Matter Physics* **10**, 409 (2019).
- [36] M. U. Ubbens and P. A. Lee, Spin-gap formation in bilayer cuprates due to enhanced interlayer pairing, *Phys. Rev. B* **50**, 438 (1994).
- [37] K. Kuboki and P. A. Lee, Energy gap structure in bilayer oxide superconductors, *Journal of the Physical Society of Japan* **64**, 3179 (1995).
- [38] J. Maly, D. Z. Liu, and K. Levin, Superconducting order parameter symmetry in multilayer cuprates, *Phys. Rev. B* **53**, 6786 (1996).
- [39] A. Nazarenko and E. Dagotto, Hole dispersion and symmetry of the superconducting order parameter for underdoped CuO_2 bilayers and the three-dimensional antiferromagnets, *Physical Review B* **54**, 13158 (1996).
- [40] A. Medhi, S. Basu, and C. Kadowaki, Phase diagram for a t - J bilayer: role of interlayer couplings, *The European Physical Journal B* **72**, 583 (2009).
- [41] A. Bohrdt, L. Homeier, C. Reinmoser, E. Demler, and F. Grusdt, Exploration of doped quantum magnets with ultracold atoms, *Annals of Physics* **435**, 168651 (2021).
- [42] A. Bohrdt, L. Homeier, I. Bloch, E. Demler, and F. Grusdt, Strong pairing in mixed-dimensional bilayer antiferromagnetic mott insulators, *Nature Physics* **18**, 651 (2022).
- [43] S. Hirthe, T. Chalopin, D. Bourgund, P. Bojović, A. Bohrdt, E. Demler, F. Grusdt, I. Bloch, and T. A. Hilker, Magnetically mediated hole pairing in fermionic ladders of ultracold atoms, *Nature* **613**, 463 (2023).
- [44] R. Eder, Y. Ohta, and S. Maekawa, Ground-state properties and dynamics of the bilayer t - J model, *Physical Review B* **52**, 7708 (1995).
- [45] M. Vojta and K. W. Becker, Doped bilayer antiferromagnets: Hole dynamics on both sides of a magnetic ordering transition, *Phys. Rev. B* **60**, 15201 (1999).
- [46] H. Zhao and J. R. Engelbrecht, t - J model for a bilayer: Coexisting superconductivity and planar-flux phases, *Phys. Rev. B* **71**, 054508 (2005).
- [47] M. Zegrodnik and J. Spalek, Effect of interlayer processes on the superconducting state within the t - J - U model: Full gutzwiller wave-function solution and relation to experiment, *Phys. Rev. B* **95**, 024507 (2017).
- [48] G. Kotliar and J. Liu, Superexchange mechanism and d -wave superconductivity, *Phys. Rev. B* **38**, 5142 (1988).
- [49] P. A. Lee, N. Nagaosa, and X.-G. Wen, Doping a mott insulator: Physics of high-temperature superconductivity, *Rev. Mod. Phys.* **78**, 17 (2006).
- [50] V. Pardo and W. E. Pickett, Metal-insulator transition in layered nickelates $\text{La}_3\text{Ni}_2\text{O}_{7-\delta}$ ($\delta = 0.0, 0.5, 1$), *Phys. Rev. B* **83**, 245128 (2011).